Analysis of a dry friction problem under small displacements: application to a bolted joint

J.F. Ferrero [b,*], E. Yettou [a], J.J. Barrau [b], S. Rivallant [a]

[a] *ENSAE-LMS, 10 Av. E. Belin, 31055 Toulouse, France*
[b] *UPS-IGM-LGMT, Bât 3PN, 118 Rte de Narbonne, 31400 Toulouse, France*

Received 11 March 2003; received in revised form 30 July 2003; accepted 30 July 2003

Abstract

This study presents an analysis of the problem of macroscopic contact of steel upon steel with dry friction, in the specific case of a bolted joint. The configurations of these types of joints result in very small displacements and interface sliding velocities. To understand how the system formed by the two surfaces in contact works, an experiment was carried out. The analysis of the results obtained made it possible to define the behavior of the system and to model the variations of the main parameters by original and continuous laws. These laws accurately correlate to all the results of the tests effectuated.

Keywords: Dry friction; Non-linear; Bolted joint; Experimental model; Numerical method

1. Introduction

The following study deals with the analysis of a macroscopic problem of a plane-upon-plane contact between two pieces of steel, with dry friction, in the specific case of a bolted joint. It is of particular interest to analyze this configuration, which can be found in a number of industrial mechanisms whenever a system prevents full sliding of the friction areas, i.e. riveted joints and shrink fitted assemblies. For this type of joint, mechanical and vibratory behavior are mainly determined by the dry friction phenomenon in the specific situation of very low interface displacement ($<100\,\mu m$) and almost non-existent sliding velocity ($<0.2\,\mu m\,s^{-1}$).

The phenomenon of contact with dry friction is difficult to model as it involves a large number of parameters interconnected by such complex relations that a universal model does not exist. Many theoretical and experimental studies have tried to define the characteristics of the variables governing the phenomenon. Firstly, the classical laws given by Coulomb [1] differentiate between static and dynamic friction coefficients and analyze the influence of parameters likely to condition their value. Secondly, are laws based on the adherence of surfaces, the best-known being the law defined by Bowden and Tabor [2,3], which explains the phenomenon of friction in metals by the adhesion and shear of junctions formed under the effect of contact pressure. This theory was further developed by Rubenstein and Tabor [4,5], who considered the plastic behavior of micro-contacts under tangential load. Other studies include work on the factors influencing the behavior of surfaces under dry friction and the increase in the static coefficient in relation to contact time. Indeed, when conditions include a blocked interface, the resulting friction coefficient would appear to depend on contact time. This can be explained by the development of the junctions which are created at the interface. Various laws are proposed [5–7], mainly differing in the speed of convergence towards the limit values, i.e. the values of the static and dynamic friction coefficients. Brockley and Davis [5] have also introduced a term to quantify the influence of temperature. Other works investigate the influence of the sliding distance of the interface. Rabinowicz [8], followed by Rigney and Hirth [9], have observed that the friction coefficient value converges towards a lower limit when sliding distance is increased. Finally, other work has analyzed the influence of sliding conditions and temperature [10,11]. For a dry steel contact, Lim et al. [12] mapped the value of the friction coefficient during sliding for a wide range of friction conditions. For high sliding velocities, the value of the friction coefficient depends on the pressure on the surface and the sliding velocity. When sliding velocities are very low and the sliding distance almost nil, the experimental study of Ferrero and Barrau [13] led to their proposal of a continuous law of variation of the friction coefficient between two asymptotic limits.

* Corresponding author.
E-mail address: jean-francois.ferrero@supaero.fr (J.F. Ferrero).

These results were obtained under particular conditions in which normal and tangential loads were linked. This is no longer so with the bolted joint. To validate these results when normal and tangential loads vary independently of one another, a new experimental study was therefore carried out.

2. Experimental method

2.1. Experimental system

An experimental model equivalent to the principle of a bolted joint was developed (cf. Fig. 1). It is composed of two steel parts (HV: 215, UTS: 710 MPa, R_a: 1.6). The lower element is a solid, linked to the loading system by means of a ball-and-socket joint. The upper element is made up of three steel plates: two vertical plates in contact with the lower element, and one horizontal plate also linked to the excitation system. To ensure that the surfaces under contact are well aligned, these three plates are attached together by screws and conical washers. The lower element is connected to the upper element in two places: at the two friction interfaces and by a load sensor allowing the tangential load F_{TC} to be controlled. The location of the sensor restricts the movement of the interface to the point of sensor deformation and thus enables very small displacements to be made. The normal load F_N is introduced by means of a nut and bolt assembly and is evaluated during the experiment using strain gauges. Both the surface and the state of the surface can be modified. The external load F_M is applied to the system using a fatigue machine. The loading velocity is low (approximately $100\,N\,s^{-1}$). The load sensor is a steel tube equipped with a complete gauge bridge. This type of sensor enables high rigidity, an essential factor if displacements at the interface are to be within the required range. The sensor has been calibrated. At each test, a simultaneous recording is made of: the load F_M applied to the system; the deformation of the sensors giving the normal contact load F_N; and the tangential load at the interface F_{TC}. Moreover, a laser displacement sensor is used to monitor the displacements of the interface. For every test, a pre-loading phase of sinusoidal type is effectuated with an amplitude of 5 kN and a frequency of 0.1 Hz, for a duration of 2 min, in order to initialize the system. Several types of load—linear or sinusoidal, surface state or normal load value—were tested to validate the models proposed.

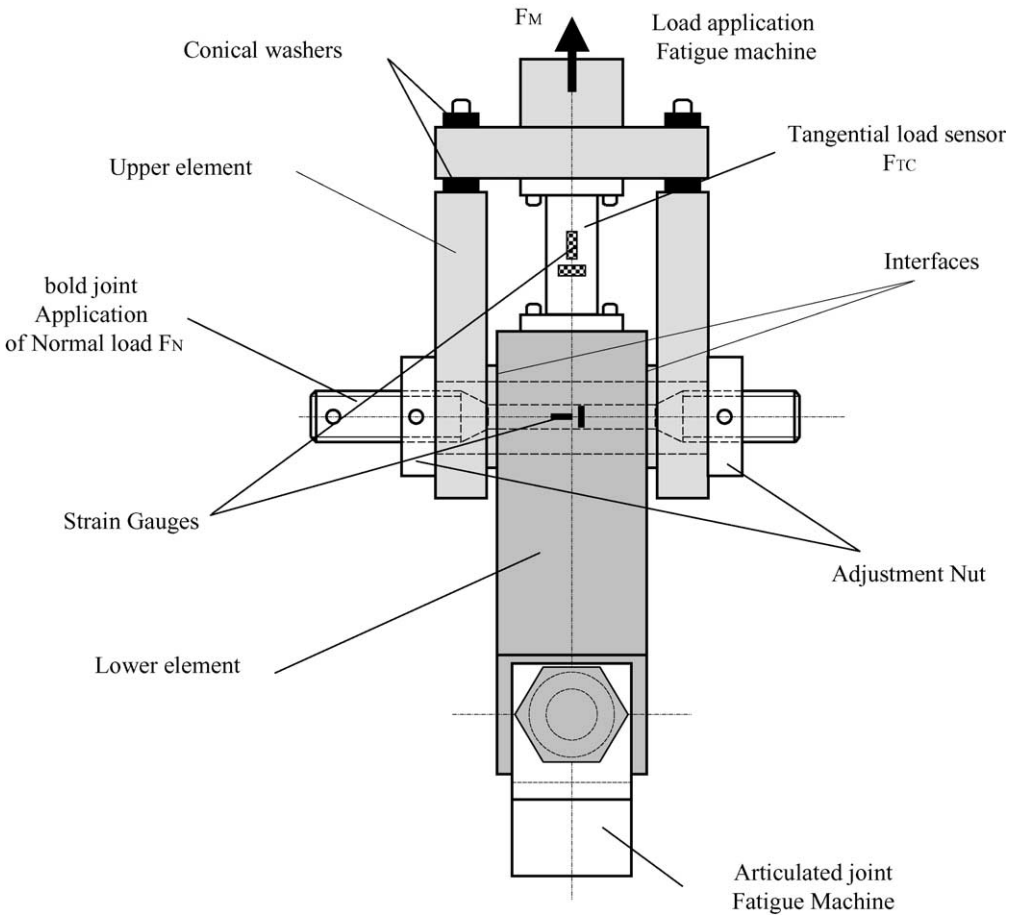

Fig. 1. Experimental system.

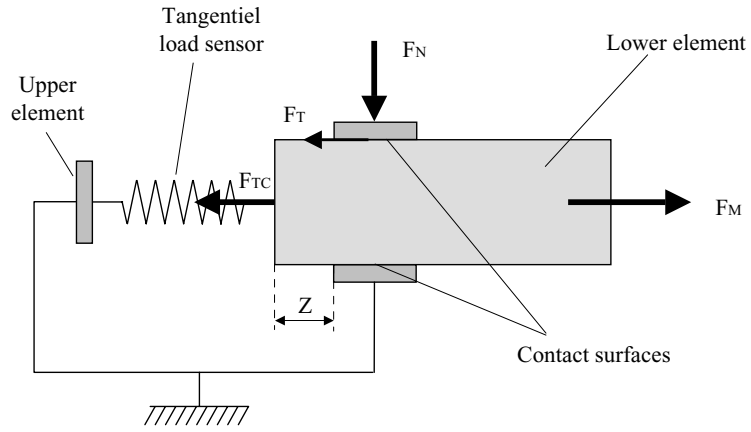

Fig. 2. Modeling of test assembly.

2.2. Modeling of the experimental system

The experimental system can be modeled as shown in Fig. 2. Because of the rigidity of the upper elements the structure can be considered as rigid. Thanks to this hypothesis, the load sensor enables us to obtain the displacements. Comparisons with measurements taken with a laser displacement sensor show that the hypothesis is valid.

To determine tangential load at the interface during sliding, it is simply necessary to record the equilibrium of the mobile part. Since the displacement velocities are negligible, the inertia loads can logically be disregarded.

It is assumed that symmetry causes the contact loads to be the same on both sides of the mobile element, thus

$$F_{\mathrm{T}} = \tfrac{1}{2}(F_{\mathrm{M}} - F_{\mathrm{TC}}) \tag{1}$$

where F_{M} is the imposed external load and F_{TC} the load measured on the sensor.

3. Results and discussion

Initially, the system is submitted to an external load (F_{M}) which varies linearly with time (see Fig. 3) for several values of normal loads 2, 4 and 6 kN. The load F_{M} increases progressively from 0 to 16 000 N between the instants t_0 and t_1 and is then decreased until zero load in t_2.

3.1. Behavior of interface loads

Fig. 3 shows the evolution of the load in the sensor with time, for three values of the normal load F_{N}. External load is zero at instant t_0, at its maximum at instant t_1, and has returned to zero at instant t_2. For the three values of the normal load, similar behavior is observed when the load increases progressively from 0 to 16 000 N. At first, the load measured in the sensor increases slowly (parts AA_1, AA_2, AA_3), before speeding up and reaching its maximum value when the external load is also at its highest. During the decreasing phase of F_{M}, two different behaviors are observed. At first, the load in the sensor varies slightly. The slope of curve and the lengths of these lines (B_iC_i) are different and depend on the normal load applied. Subsequently, the load measured on the sensor decreases very rapidly but does not return to zero.

3.2. Analysis of the results

The analysis of the curves in Fig. 3 shows that:

- During the loading phase (AB), the interface goes from a quasi-static state (AA_i) to a sliding state (A_iB_i). This is classical and follows standard theories of friction.
- The larger the normal load, the higher the tangential load must be in order for sliding to occur. On the other hand, accurate analysis of the sliding element (cf. Fig. 4) shows that the friction coefficient is not constant as predicted in the classical theory, but varies during the sliding phase.
- During the unloading phase the interface is in a quasi-static state as soon as the external load decreases. Once the value of the external load is weak enough, the interface goes from a quasi-static state to a sliding state if the load in the sensor is enough to push back the moving element. It is worth noting that during the quasi-static state the rigidity of the interface depends on the normal load applied.

These tests clearly demonstrate that no classical laws characterize the evolution of the friction interface completely.

To model the phenomena observed in these first tests, which corroborate results observed in [13], we suppose that the friction interface can be modeled as in [14] using a spring during quasi-static phases and a slide pad during sliding states of the interface, since both these elements have specific behavior. In the event of a quasi-nonexistent sliding velocity we have made the hypothesis, as in [13], that sliding distance is the determining parameter in the variation of the friction coefficient during states of micro-sliding.

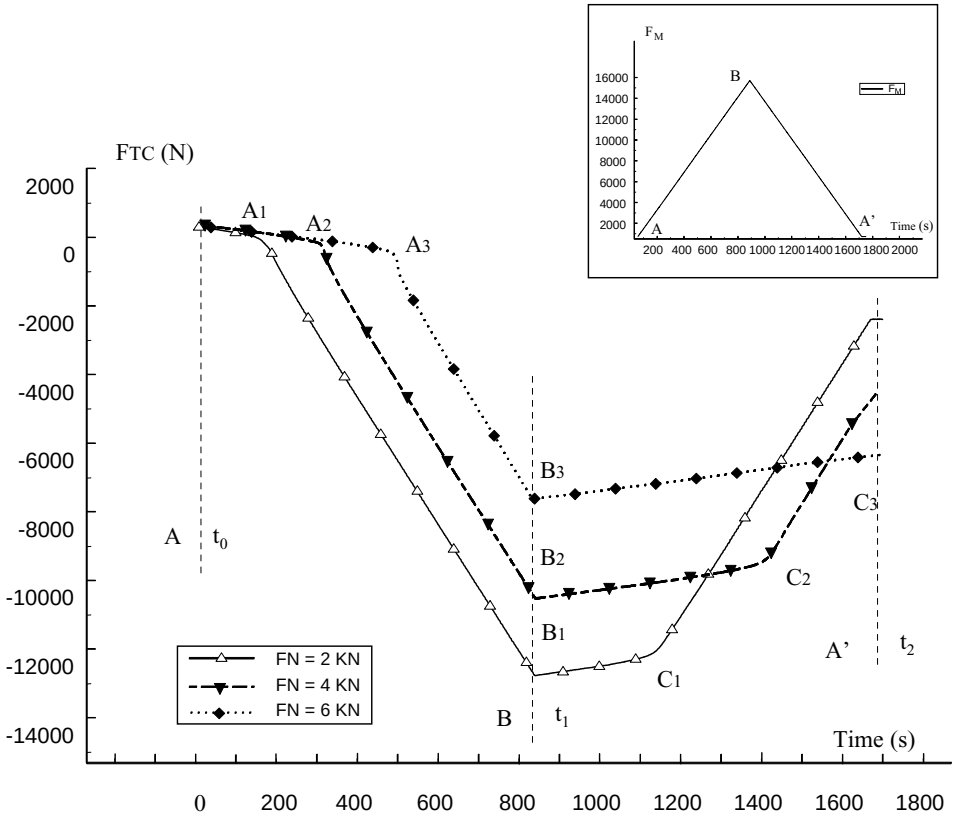

Fig. 3. Variation of the load in the sensor.

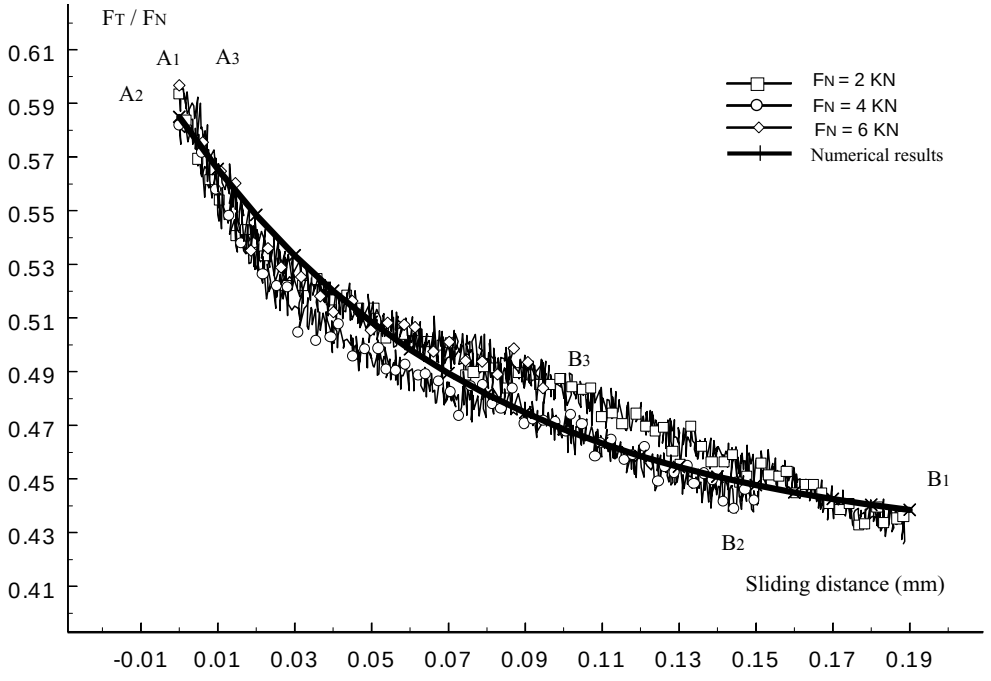

Fig. 4. Friction coefficient/sliding distance relationship.

The variations of this coefficient with sliding distance (cf. Fig. 4) show that it appears to follow an exponential law of friction when evolving between a maximum value corresponding to the friction coefficient value at the beginning of the sliding state and a minimum value at the end of the sliding state. These two values are limited by two asymptotic boundaries, the maximum one corresponding to the static value and the minimum one to the dynamic value of the friction coefficient.

This behavior is modeled, as in [14], by the following law:

$$\mu = \mu_{\mathrm{d}} + (\mu_{\mathrm{c}} - \mu_{\mathrm{d}})\,\mathrm{e}^{-Cq} \tag{2}$$

in which μ_{d} is the minimum asymptotic value, corresponds to the value usually interpreted as the dynamic value of the friction coefficient. μ_{c} is the maximum value during the sliding phase, its value being linked to the end of the previous blocked state. It ensures the continuity of the variation in the blocked state/sliding state direction and depends on the case history of the interface. q is the sliding distance; C is a constant. For the studied case, constant C has a value between 12 and 16. It controls the transition from μ_{c} to μ_{d}. Referring to experimental tests, it was noticed that the value of C varies with the interface characteristics.

During quasi-static states of the interface (AA_i) and ($\mathrm{B}_i\mathrm{C}_i$), the tangential micro-displacements observed are near-linear functions of the tangential load applied. This behavior is reversible and is determined by a tangential contact rigidity. Analysis of the system's reaction during the two blocked states (cf. Fig. 3) shows that the curves of the graph representing the variation of F_{TC} differ according to the intensity of the normal load. The same result occurred with all the tests effectuated.

Fig. 5 represents the evolution of the interface rigidity with the normal load applied to the system. Unlike [14] in which normal load varied with tangential loading, these results lead us to suppose that

$$k_{\mathrm{r}} = k\sqrt{F_{\mathrm{N}}} \tag{3}$$

where F_{N} is the normal load applied.

This phenomenon can be explained in physical terms as follows: as the intensity of the normal load varies, so does the number of joints between junctions on the interface. Another important phenomenon is the influence of the case history of the interface upon the evolution of the value of the coefficient. To study this influence, various types of tests were carried out. For instance, the joint is first loaded in compression by progressively varying the load force from 0 N up to 7.5 kN. A sinusoidal excitation with an amplitude of 2 kN and a frequency of 0.1 Hz is then applied. So as to increase the duration of the quasi-static state, the number of cycles is progressively modified from 1 to 180, i.e. a quasi-static contact time ranging from 10 to 1800 s. This phase is followed by a large increase in the compression load (up to 15 kN) so as to force the interface into a sliding state. The system is then completely unloaded. Fig. 6 shows the evolution of the load in the sensor and the external load for 120 cycles. The curve illustrates that during sinusoidal excitement the system is in a quasi-static state and its reaction is perfectly represented when studying the rigidity k of the interface. It is interesting to look into how the relationship $F_{\mathrm{T}}/F_{\mathrm{N}}$ varies during the first phase of sliding, i.e.

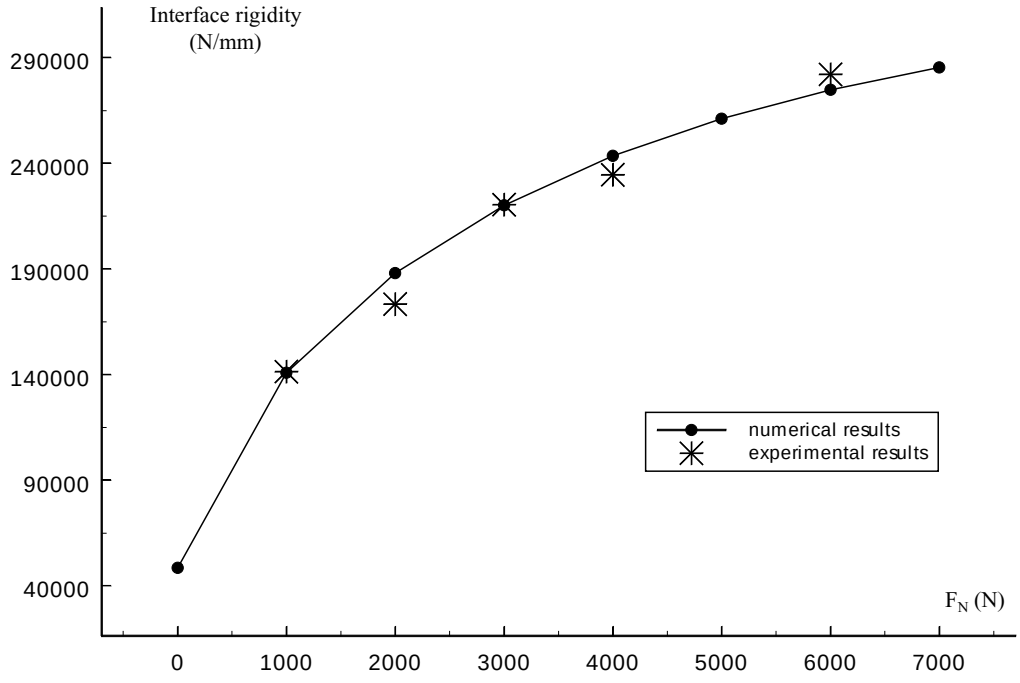

Fig. 5. Interface rigidity/normal loading relationship.

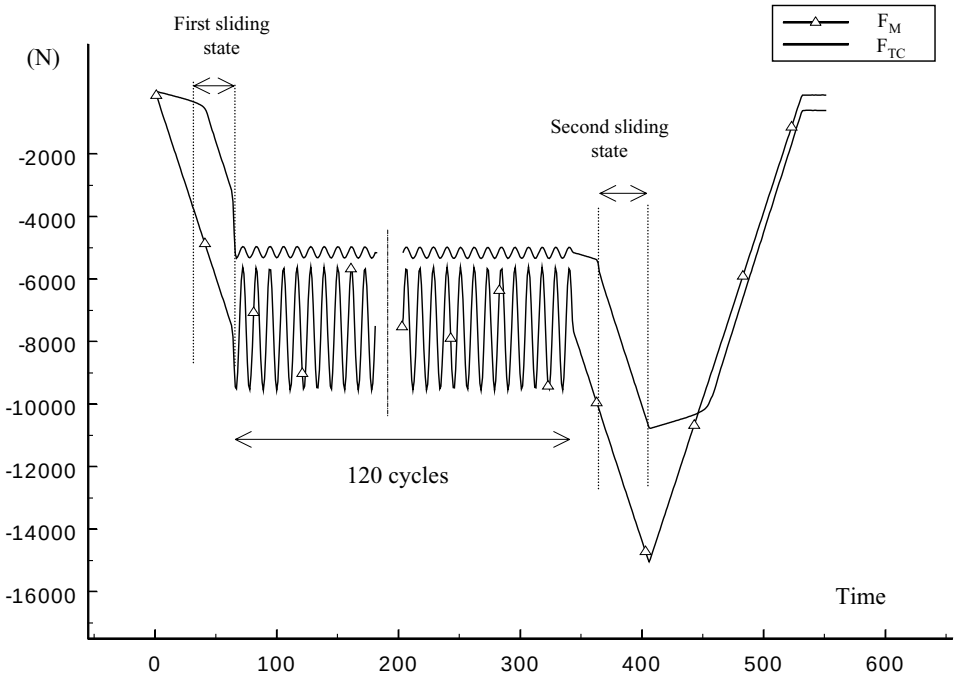

Fig. 6. F_M/F_{TC} relationship for a contact time of 1200 s.

at the beginning of loading, and during the second phase of sliding when a quasi-static phase is imposed after the sinusoidal loading. These analyses always take the sliding distance into account. In Fig. 7, the line corresponds to a normal applied load of 2 kN, a linear loading speed of 8 kN/min and a quasi-static contact time of 1200 s. During the first sliding phase the friction coefficient value diminishes from 0.56 to 0.52. It then increases during the quasi-static phase of the interface. During the second sliding state its value is 0.61 at the beginning and 0.52 at the end. Table 1 gives the percentage increase in value of the friction coefficient between the end of the first sliding state and the beginning of the second,

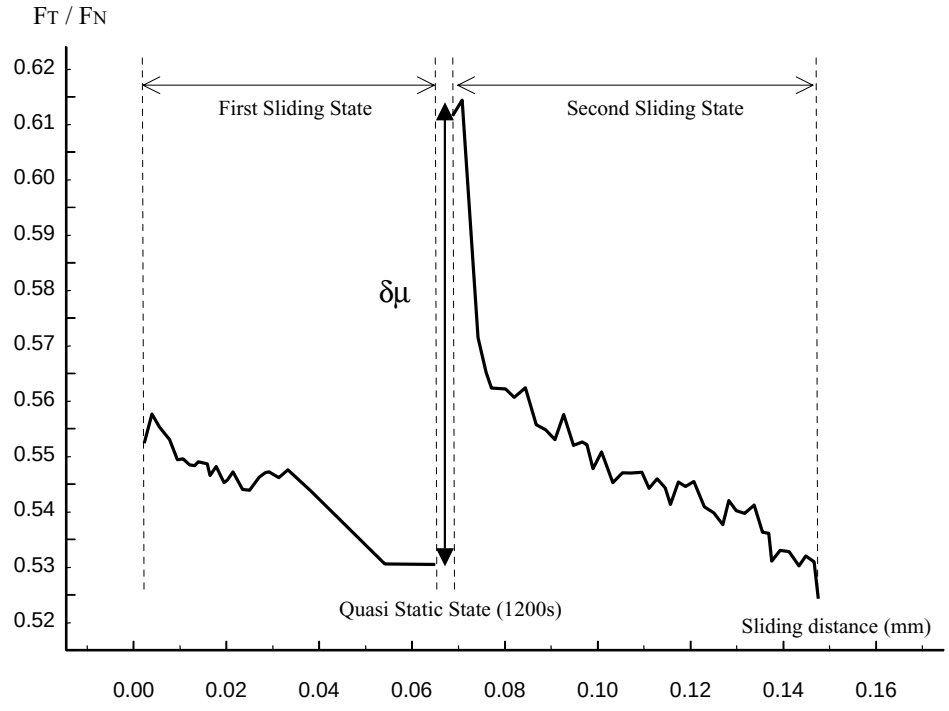

Fig. 7. Friction coefficient/sliding distance relationship for a contact time of 1200 s.

Table 1
F_T/F_N variation during the quasi-static contact time

	Contact time (s)					
	50	150	300	600	1200	1800
$(F_T/F_N)_I$	0.529	0.527	0.531	0.532	0.527	0.527
$(F_T/F_N)_{II}$	0.57	0.585	0.599	0.611	0.618	0.62
$\Delta(F_T/F_N)$ (%)	7.75	11	12.8	14.8	17.3	17.65

and for different static contact times. These results express an increase related to the duration of the quasi-static state of the interface. As in [14], we suppose that the value of the friction coefficient is linked to the quasi-static contact time (cf. Fig. 8) by the following relation:

$$\mu = \mu_s - (\mu_s - \mu_c)\, e^{-\gamma T_c^{\alpha}} \tag{4}$$

where μ_s corresponds to the value usually interpreted as the static value of the friction coefficient, μ_c is equal to the value of the friction coefficient at the end of the previous sliding state of the interface, α and γ are constants. For the studied case, the values of γ and α are 0.015 and 0.75, respectively. These constants govern the friction coefficient value during the quasi-static phase. As it was observed for the constant C, the values of α and γ are associated to the surface state and the environment.

This law enables a correct model to be made of the experimental variations observed. From these observations a model of the behavior of the interface can be made. This is a local model which uses experimental global results. This model is composed of a spring element of rigidity k linked to a dry friction joint. It is original in that the laws of variation associated to the different parameters correspond to the results obtained from experiments.

The simulation represented in Fig. 9 shows the displacement of the moving part in relation to the load introduced into the system in the case of linear loading studied in the first part and defined in Fig. 3. For the three values of normal load the numerical results obtained compare favorably with the experimental results. At the beginning of loading the interface is blocked, the response curve is controlled by the contact tangential rigidity. When the intensity of the external loading reaches a high enough level, the interface slides. The variation of the friction coefficient in relation to the sliding distance enables the experimental results to be represented well. When the load decreases the interface stops moving and is controlled by both the contact rigidity and the increase in the friction coefficient in relation to time. Then, depending on the intensity of the normal load, the elastic energy which has accumulated in the sensor pushes the moving part back to its original position. As well as the various states of the interface, the transition from one to the other is also taken into account when producing the model, both for quasi-static and for sliding states. Fig. 10 represents the modeling of a more complex load defined in Fig. 6. In this more general framework, where a quasi-static state of 1200 s is imposed between two sliding states of the interface, correct results are obtained from modeling. The increase in the friction coefficient with contact time during the quasi-static state enables the behavior of the interface to be correlated. It also makes it possible to represent the variations in displacement measured on the sensor between the end of the

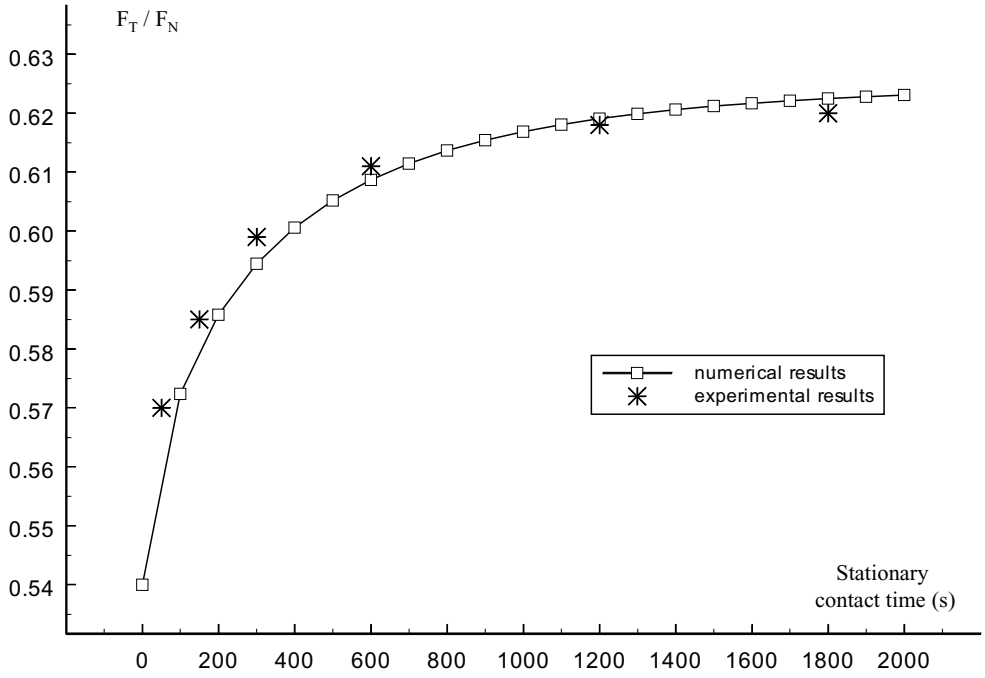

Fig. 8. Friction coefficient/quasi-static contact time relationship.

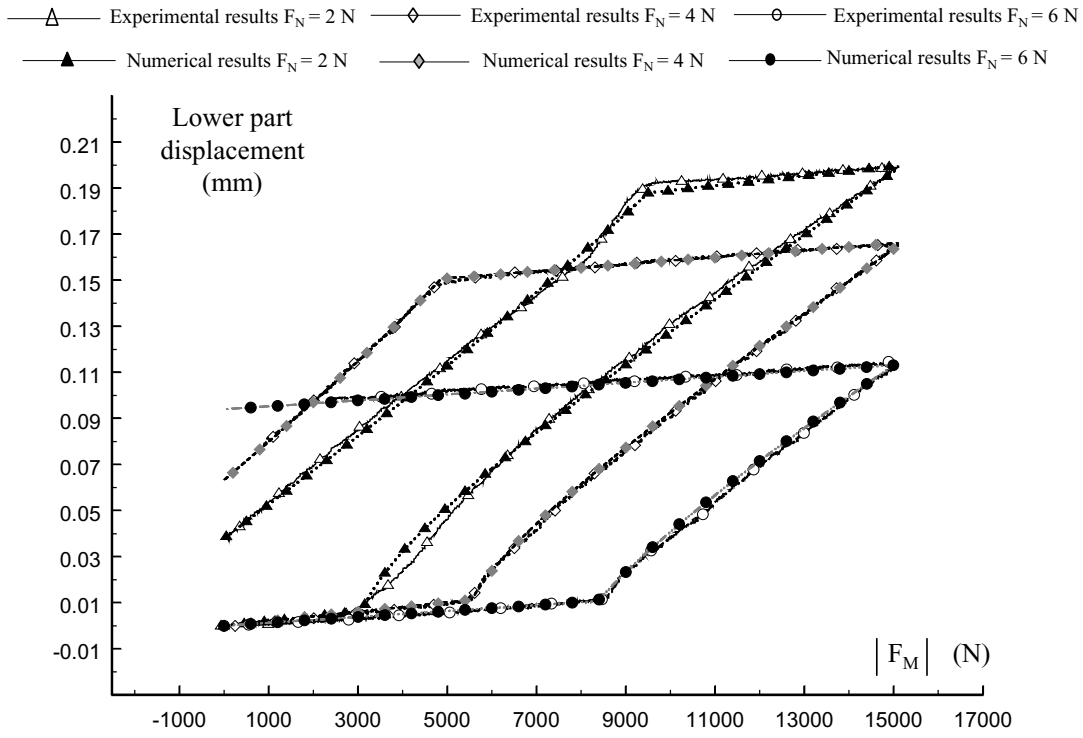

Fig. 9. Lower part displacement: experimental and numerical results.

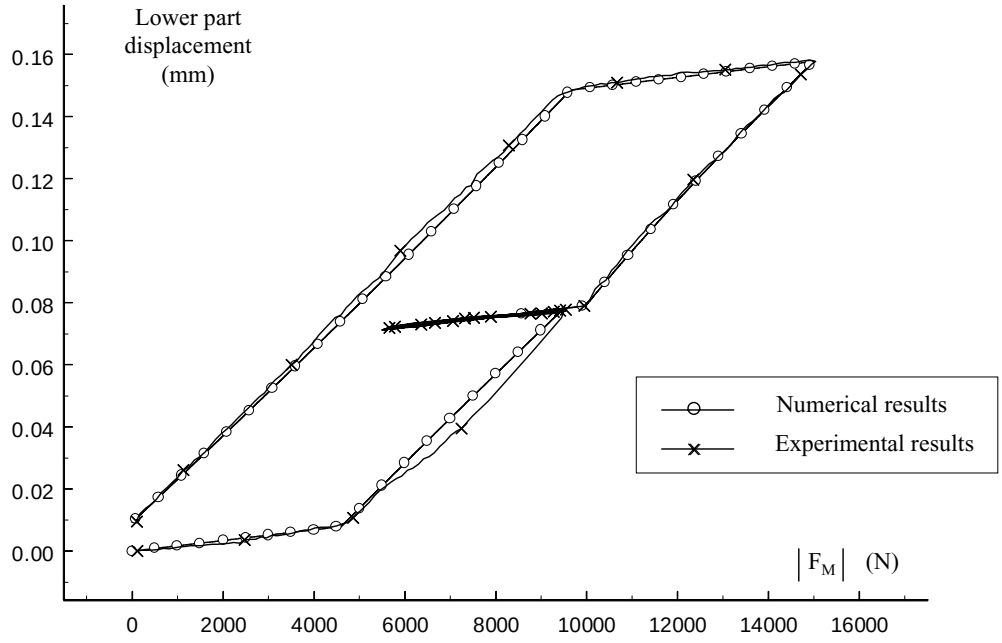

Fig. 10. Lower part displacement: experimental and numerical results.

first sliding state and the beginning of the second. The laws were defined in a specific case of friction involving linked introductions of the normal and tangential loads. These laws produce acceptable models of the variation of the main parameters which determine the behavior of the interface in the case of a bolted joint.

4. Conclusion

These results confirm the laws of variation determined in [13] by Ferrero et al. in the study of dry friction with near zero interface displacement for the more general case in which normal and tangential loads are independent of

each other, as in the case of bolted joints. These results thus show that: when an interface slides, the friction coefficient decreases, from a maximum value in relation to the sliding distance. Then, during a quasi-static state phase, its value increases in relation to the quasi-static contact time, starting from the value reached at the end of the previous sliding state. The sliding coefficient varies continuously within two asymptotic boundaries and in relation to the case history of the interface. It will only return to its static value if the contact time is long enough. Moreover, the rigidity of the interface varies with the normal load.

These experimental laws enable models to be produced for the behavior of the interface under complex loads. The calculated values correlate correctly with results obtained from experiments and correspond to the various states of the system which would appear in a continuous model of the variation of friction coefficient. Defined by three empirical laws, it is possible to integrate this model into the modeling of complex joints when surfaces in contact with each other undergo very small displacements and near zero sliding velocities. Studies are in progress to examine the validity of these laws for different interface materials and to analyze the sensitivity of the constants C, α and γ relative to the interface characteristics.

References

[1] R. Courtel, Le frottement sec Revue Française de Mécanique No. 66, 1978.

[2] F.P. Bowden, D. Tabor, The Friction and Lubrification of Solids, Clarendon Press, Oxford, 1950.

[3] D. Tabor, Friction—the present state of our understanding, J. Lubr. Technol. 103 (1981) 169, 179.

[4] V.A. Belyi, K.C. Ludema, N.K. Myshkin, Tribology in the USA and the Former Soviet Union: Studies and Applications, Allerton Press, Inc., New York, 1994.

[5] C.A. Brockley, H.R. Davis, The time-dependence of static friction, ASME J. Lubr. Technol. (USA) 90 (1) (1968) 35–41.

[6] E. Rabinowicz, Friction and Wear of Materials, Wiley, New York, 1966.

[7] R.S.H. Richardson, H. Nolle, Surface friction under time dependent loads, Wear 37 (1976) 87–101.

[8] E. Rabinowicz, The nature of the static and kinetic coefficients of friction, J. Appl. Phys. 22 (1951) 1373–1379.

[9] D.A. Rigney, J.P. Hirth, Plastic deformation and sliding friction of metals, Wear 53 (1979) 345.

[10] J.A.C. Martins, J.T. Oden, F.M.F. Simões, A study of static and kinetic friction, Int. J. Eng. Sci. 28 (1) (1990) 29–92.

[11] H.L. Armstrong, How dry friction really behaves, Am. J. Phys. 53 (9) (1985) 910–911.

[12] S.C. Lim, M.F. Ashby, J.H. Bunton, The effects of sliding conditions on the dry friction of metals, Acta Metall. (GB) 37 (3) (1989) 767–772.

[13] J.F. Ferrero, J.J. Barrau, Study of dry friction under small displacement and near-zero sliding velocity, Wear 209 (1997) 322–327.

[14] J.F. Ferrero, Contribution a l'étude du frottement sec sous faible déplacement, Application au four rotatif, These de Doctorat, ENSAE, N° d'ordre, 1996.